HYDROGEN SAFETY

Toward a Reliable Methodology for Assessing Overpressure in Hydrogen Vents

RESEARCH

JOSUE MELGUIZO-GAVILANES
ADISA JARUBENJALUK
ANDRZEJ PEKALSKI
ANDREW CRERAND
*Author affiliations can be found in the back matter of this article

KIT Scientific Publishing

hySafe
INTERNATIONAL ASSOCIATION FOR HYDROGEN SAFETY

ABSTRACT

The oil, gas, and chemical industries continually face risks from accidental releases of flammable gases, which can lead to severe consequences if ignited after a delay. Hydrogen, gaining popularity as an alternative fuel, poses specific challenges due to its explosion hazards. Ensuring safety requires a thorough understanding and prediction of gas explosion outcomes. With the anticipated increase in hydrogen production and usage in both public and industrial settings, establishing safe venting guidelines is essential. There is no industry-standard methodology for hydrogen venting that reliably estimates overpressures from deflagration and detonation, following the delayed ignition of flammable clouds. This study aims to address this gap by building on a methodology introduced in earlier works. The methodology involves determining the mass of hydrogen contributing to the blast loads in the cloud through dispersion calculations using standard consequence modeling software (e.g., FRED, PHAST) and engineering judgment. The article also discusses the limitations of the predictive capabilities of unconfined and uncongested deflagration/detonation models when tested against the available experimental data (i.e., large under-/overpredictions in overpressure estimates). An updated methodology is proposed based on a scaling that relates the vent release conditions (i.e., pressure and diameter) to the visible flame velocity in nonuniform, nonquiescent flammable clouds. A map of expected overpressures as a function of pressure and vent diameter is provided.

CORRESPONDING AUTHOR:
Josue Melguizo-Gavilanes
Shell Global Solutions B.V., Energy Transition Campus (ETCA), 1031 HW Amsterdam, The Netherlands
j.MelguizoGavilanes@shell.com

KEYWORDS:
hydrogen venting; overpressure prediction; hydrogen explosion hazards; consequence modelling

TO CITE THIS ARTICLE:
Melguizo-Gavilanes, J., Jarubenjaluk, A., Pekalski, A. and Crerand, A. (2026) 'Toward a Reliable Methodology for Assessing Overpressure in Hydrogen Vents', *Hydrogen Safety*, 3(1), pp. 63–72. Available at: https://doi.org/10.58895/hysafe.51

1. INTRODUCTION

Hydrogen venting is a critical safety process in industries where hydrogen is produced, stored, or used as fuel (Dorofeev, 2007; Melguizo-Gavilanes, Pekalski, and Crerand, 2024). As hydrogen plays a growing role in the low-carbon energy transition, managing its venting is essential to prevent overpressurization and ensure system safety. Hydrogen's low molecular weight and high diffusivity allow it to disperse quickly, reducing accumulation risks (Boivin *et al.*, 2023). However, improper venting can lead to hazards such as flammable cloud formation, delayed ignition, or hydrogen jet ignition (Schefer *et al.*, 2007). High-pressure venting creates high-velocity jets that, if ignited by static electricity, sparks, or hot surfaces, may result in jet fires. Hydrogen's wide flammability range (4–75%) and low ignition energy make it particularly prone to ignition, necessitating robust safety measures (Brennan and Molkov, 2013).

The key challenges in hydrogen venting include predicting dispersion patterns under varying environmental conditions (e.g., wind, temperature, humidity) (Venetsanos, Papanikolaou, and Bartzis, 2010) and mitigating ignition risks. Tools such as Shell FRED (Fire Release Explosion Dispersion) and PHAST (Professional, Process Hazard Analysis Software Tool) provide initial dispersion modeling. At the same time, vent system designs must incorporate safety measures such as grounding, bonding, and flame arrestors (Astbury and Hawksworth, 2007). A significant concern is delayed ignition, where dispersed hydrogen clouds ignite after encountering a distant ignition source, potentially causing deflagration or even detonation under certain conditions (Chamberlain, Oran, and Pekalski, 2019; Thomas, Eastwood, and Goodrich, 2015; Oran, Chamberlain, and Pekalski, 2020). While vent releases into open air typically reduce explosion risks due to minimal congestion, it is argued that hydrogen's high burning rate may still generate damaging overpressures in turbulent conditions (Groethe *et al.*, 2007; Miller, Eastwood, and Thomas, 2015).

Industry standards, such as API 521 (Standard, 2020), focus on thermal radiation safety but may not adequately address overpressure risks from hydrogen venting. For instance, a worker beneath a vent stack designed to meet thermal radiation guidelines may still face unsafe overpressure levels if ignition occurs. This highlights the need for reliable models to predict overpressures during venting.

This article builds on the methodology first introduced in the work of Melguizo-Gavilanes, Pekalski, and Crerand (2024) that has been revisited by Dorofeev (2007). The limitations of the predictive capabilities of unconfined and uncongested deflagration/detonation models when tested against available experimental data are addressed (i.e., large under-/overpredictions in overpressure estimates). An updated methodology is proposed based on a scaling that relates the vent release conditions (i.e., pressure and diameter) to the visible flame velocity in nonuniform, nonquiescent flammable clouds. The magnitude of the resulting overpressure estimates is in agreement with experimentally reported values.

2. METHODOLOGY

This section introduces the methodology, which comprises a dispersion calculation and the use of correlations to compute overpressures or blast loads from unconfined and uncongested deflagrations and detonations. It was first introduced in the work of Melguizo-Gavilanes, Pekalski, and Crerand (2024) and is included below for completeness.

2.1. DISPERSION

The dispersion contours can be estimated for the actual composition in the vent using the pressurized release scenario in Shell FRED or using any other standard consequence modeling software such as PHAST. This information is useful to estimate the total mass/volume of gas present in the cloud between lower flammability limit (LFL) and upper flammability limit (UFL), or other relevant contours, in particular, the mass of H_2 that is likely to contribute to the overpressure in case of delayed ignition of the H_2-air cloud. Note that it is the available mass of H_2 that determines the total (potential) combustion energy that can be released. This is a key input parameter required for the correlations used to estimate the expected overpressures from deflagrations or detonations that is presented as follows.

DOI: 10.58895/hysafe.51

The external environment conditions are also an important input to the model. For vertical releases and expected configuration of vents, care must be taken when the exit velocities are comparable to typical wind speeds in the area where the vent is to be operating.

2.2. OVERPRESSURE: UNCONFINED DEFLAGRATION CASE

An appropriate description for the blast loads induced by deflagrations should necessarily include the flame speed as the pushing of the gas ahead of the flame is responsible for the pressure buildup. The overpressure at the cloud boundary can be obtained by a quasi-acoustic approximation, which yields the following expression for overpressure:

$$P_2^* = \left(\frac{V_f}{a_0}\right)^2 \frac{\sigma - 1}{\sigma} \left(\frac{0.83}{R^*} - \frac{0.14}{R^{*2}}\right) \text{ valid for } 0.21 < R^* < 3.77 \text{ and } V_f \leq 500 m/s \quad (1)$$

The coefficients are applicable to air explosions. The parameters $P^* = \Delta p/p_0$ and $R^* = R(p_0/E)^{1/3}$ are referred to as Sachs variables and represent a scaled overpressure and distance, where R denotes the radius from the blast epicenter. $\Delta p = p - p_0$ is the overpressure, p_0 is the ambient pressure, and E is the total combustion energy released.[1] The latter is a function of the type and mass of fuel present in the cloud. Additional details about this correlation can be found in Dorofeev's papers (2007, 1995). V_f denotes the visible flame speed or flame speed in the laboratory frame of reference, σ is the expansion ratio, and a_0 the sound speed in air (353 m/s at 300 K). Note that the prediction of turbulent flame speeds V_f for given initial and boundary conditions is a rather complex problem; however, an estimate for the increase in V_f with distance R for freely propagating flames based on fundamental combustion properties (FCP) can be suggested (Dorofeev, 2007).

$$V_f = A\sigma(\sigma - 1)s_L \left(\frac{R}{\delta}\right)^{1/3} \quad (2)$$

Here, $A = 8.5 \times 10^{-3}$ is an empirical parameter obtained via least-squares regression by fitting experimental data for various fuel–air mixtures to the functional form mentioned above. The remaining variables are FCP, namely, s_L which indicates the laminar burning velocity and $\delta = \nu/s_L$ which indicates the laminar flame thickness with ν denoting the momentum diffusivity or kinematic viscosity of the reactive gas. The FCP are a function of stoichiometry or fuel concentration and can be computed using thermochemical packages such as that provided by Cantera (Goodwin *et al*., 2023), together with a detailed chemical mechanism like GRI-Mech 3.0 (Smith *et al*., 2021). This is shown in Figure 1.

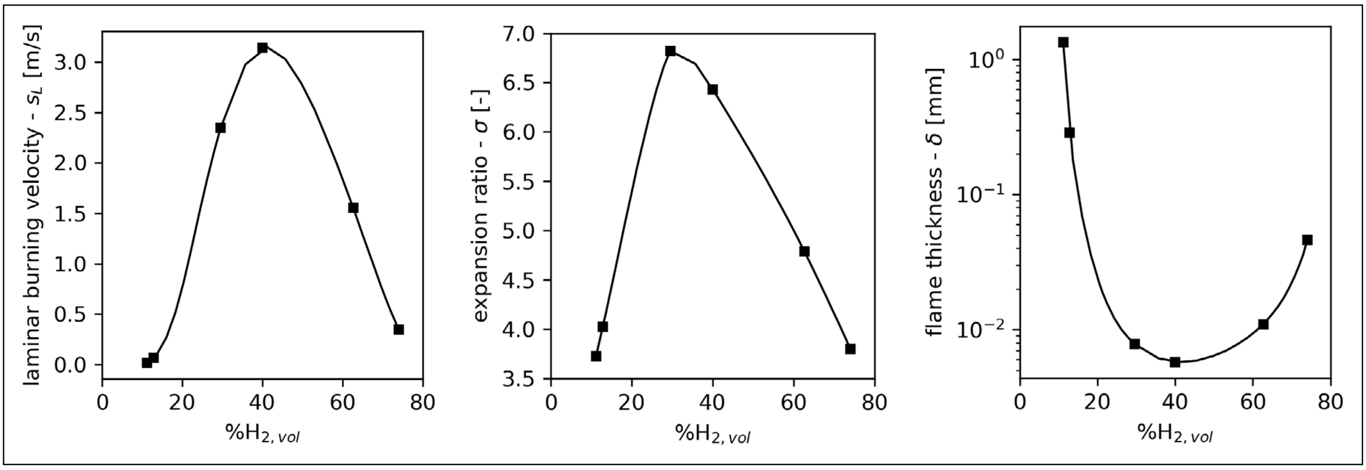

Figure 1 Laminar burning velocity, expansion ratio, and laminar flame thickness as a function of %$H_{2,vol}$ in air. Markers are shown for 11.2, 12.8, 19.6, 40.1, 62.7, and 74 %$H_{2,vol}$. Initial conditions: p_0 = 100 kPa and T_0 = 300 K.

For H_2-air mixtures at ambient pressure and temperature, s_L exhibits a lower and upper limit of 0.014 m/s and 3.14 m/s at %$H_{2,vol}$ of 11.2 and 40, respectively; σ is bounded between 3.73 at %$H_{2,vol}$ = 11.2, and 6.82 at %$H_{2,vol}$ = 29.6; δ shows a minimum at %$H_{2,vol}$ = 40 (5.76×10^{-3} mm) and a maximum at %$H_{2,vol}$ = 11.2 (1.33 mm).

1 Potential for energy release based on the mass of H_2 available in cloud and lower heating value of the fuel (LHV); LHV = 120 MJ/kg H_2.

DOI: 10.58895/hysafe.51

An added complexity in realistic releases is that the resulting clouds are nonuniform. Thus, their eventual delayed ignition would result in spatially dependent visible flame velocities, V_f. However, the correlations discussed include a single value of the FCP to be used as inputs. Approaches using varying degrees of complexity can be thought of to arrive at sensible values to use, such as defining average values accounting for the FCP dependence on stoichiometry by integrating over the volume of the cloud and invoking some simplifying assumptions[2] or using computational fluid dynamics (CFD). For the latter, the length and time scales of industrial interest may render the use of CFD intractable at present. Here, for simplicity, an arithmetic average based on the dependencies shown in Figure 1 for $\%H_{2,vol} \geq 29.6$ is deemed as sufficient.

Figure 2 (left) shows the predicted V_f as a function of distance predicted by Equation 2. Note that in the range of $\%H_{2,vol}$ present in reactive clouds, V_f can easily span four orders of magnitude. The lower bound corresponds to 11.2 $\%H_{2,vol}$ whereas the upper bound is given by 40.1 $\%H_{2,vol}$. The dashed line in the figure shows the result obtained using the arithmetic average of the FCP mentioned above, i.e., s_L = 1.85 m/s, σ = 5.46, and δ = 1.76 × 10⁻² mm. The markers show experimental results from Pförtner and Schneider (1983) (squares) and Groethe *et al*. (2007) (circle – one data point) for unconfined deflagrations in quiescent stoichiometric H_2-air (29.6 $\%H_{2,vol}$) ignited in a hemispherical plastic envelope which was cut before ignition. V_f values of 40, 78, 80, and 80 m/s are reported at distances of 3, 5.23, 10, and 14 m, respectively, from ignition. Equation 2 yields 57, 69, 85, and 96 m/s at the same distances. Figure 2 (right) shows the overpressure predictions for deflagrations (quiescent 29.6 $\%H_{2,vol}$ uniform flammable cloud) containing a mass of hydrogen of approximately 51 kg in a hemisphere of radius R = 10 m. The maximum overpressure recorded in the air blast wave was about 6 kPa; the maximum overpressure given by Equation 1 is 6.21 kPa, which is in good agreement with the experimental data.

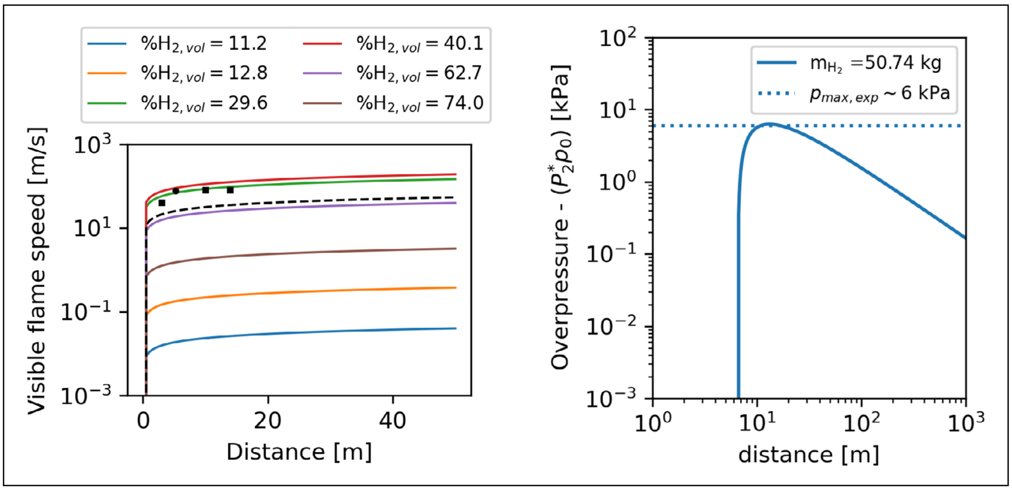

Figure 2 Left: Visible flame speed V_f versus distance computed with Equation 2 for varying H_2 content in air. Initial conditions: p_0 = 100 kPa and T_0 = 300 K. Dashed line shows the results for the arithmetic average of FCP for $\%H_{2,vol} \geq 29.6$. Square and circular markers are experimental data points for a hemisphere filled with 29.6 $\%H_{2,vol}$ taken from Pförtner and Schneider (1983) and computed using data from Groethe *et al*. (2007), respectively. Right: Predicted (Equation 1) and maximum measured overpressure for experimental configuration in Pförtner and Schneider (1983).

2.3. OVERPRESSURE: UNCONFINED DETONATION CASE

The following correlation can be used for estimating the far-field relative maximum overpressure of a blast wave created by a vapor cloud detonation in open space (Dorofeev, 2007, 1995).

$$P_1^* = \frac{0.34}{R^{*4/3}} + \frac{0.062}{R^{*2}} + \frac{0.0033}{R^{*3}} \text{ valid for } 0.21 < R^* < 3.77 \quad (3)$$

The Sachs variables defined in the previous section remain valid.

While an unconfined detonation defines an upper bound of the overpressure effect, the direct initiation of detonations is not a very probable event in industrial accidents, as energy deposition typical of high explosives is required. Detonations may plausibly occur as a result of the accidental ignition of a flammable cloud, the formation of a flame, and its subsequent acceleration and transition to detonation within the cloud. For uncongested and unconfined

2 H_2 releases form a hemispherical cloud with a nonuniform concentration having its maximum C_{max} at the center of the cloud and decreasing linearly toward the edge. Cloud properties are fully defined by C_{max} and total mass of H_2 in the cloud.

releases, two flame acceleration mechanisms come to mind. The first is intrinsic flame instabilities due to the expansion of burnt gases (Darrieus–Landau instability) and heat and mass diffusion taking place at different rates across the flame surface (thermo-diffusive); the latter is quite prominent in lean H_2 mixtures. The second factor is the interaction of the flame with the background turbulence generated by the release. These mechanisms, however, are not as effective as congestion in leading to a substantial increase in flame surface area and burning rate, and therefore to strong flame acceleration within the cloud, such that V_f values on the order of a few hundred m/s can be attained.

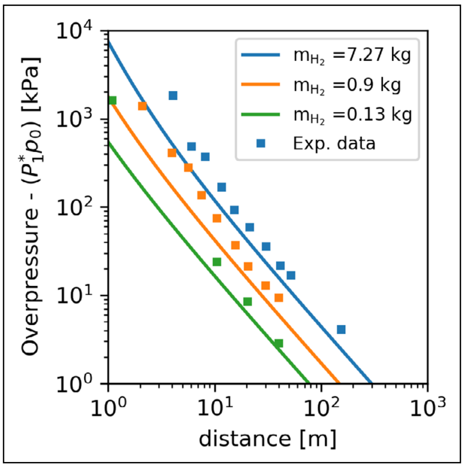

Figure 3 Predicted (Equation 3) and measured overpressure as a function of distance *R*. Square markers are experimental data points for a 300 m³ hemisphere filled with a stoichiometric H_2-air mixture (~30 $\%H_{2,vol}$) taken from Groethe *et al*. (2007). Initial conditions: p_0 = 100 kPa and T_0 = 300 K.

To validate the correlation above, the experiments of Groethe *et al*. (2007) are used, in which 300, 37, and 5.2 m³ of quiescent premixed stoichiometric H_2-air contained in a hemispherical plastic tent that was cut prior to ignition were detonated using a high explosive. In these idealized configurations, the mass of H_2 present in the cloud is known, approximately 7.3, 0.9, and 0.13 kg H_2, respectively. The total combustion energy released, *E*, is therefore a key input to the model. The results are shown in Figure 3. The agreement with the measured data is satisfactory.

For the nonuniform clouds typical of realistic releases, the accurate determination of *E* is not so straightforward since the amount of fuel present in the cloud that contributes to the blast load needs to be estimated. Here, for simplicity, it will be assumed that H_2-air mixtures at ambient conditions (100 kPa and 273 K) are detonable in the range of 12–74$\%H_{2,vol}$ (Stamps *et al*., 1991). The choice is motivated by the sharp increase in cell sizes measured in tubes between 14 $\%H_{2,vol}$ and 13 $\%H_{2,vol}$ signaling the presence of a limit around these values (Kaneshige and Shepherd, 1997); the cell size is an intrinsic length scale in detonations used to characterize them. However, it is important to note that detonability limits are not fixed values of mixture composition but depend on the ratio of a length scale dictated by the geometry of the system to the cell size. For a more complete discussion on detonability limits for nonuniform clouds and the concept of a limiting cell size gradient, see the work of Bauwens, and Dorofeev (2020). In the parametric study, the mass of H_2 used for computing unconfined detonation blast loads will be that given by a dispersion calculation between the 12 and74 $\%H_{2,vol}$ contours, whereas for the deflagration case, the mass of H_2 present in the entire flammable range will be used. Furthermore, it will be assumed that the entire mass of H_2 contributes to the blast load.

3. RESULTS AND DISCUSSION

3.1. VENT CONDITIONS AND EXTERNAL ENVIRONMENT

The venting of pure H_2 through headers of diameter *d* = 0.3–0.6 m and vent pressures of *p* = 1.3–2 bara at a height of 15 m are considered. Temperature is assumed to be 313 K (40ºC). A total of 64 simulations are run covering this parametric space. The ambient pressure, temperature, and relative humidity are set to 101.325 kPa (1 bara), 288 K (15ºC), and 70%, respectively, with a wind speed of 5 m/s. The meteorological conditions defining the Pasquill stability class correspond to slight daytime insolation and overcast nighttime conditions (i.e., D-Neutral).

Hydrogen Safety
DOI: 10.58895/hysafe.51

3.2. DISPERSION RESULTS

Figure 4 shows heat maps of relevant selected metrics from steady-state dispersion calculations carried out in FRED: namely, the vent mass flow rate (kg/s), mass of H_2 between LFL and UFL (kg), and the mass of H_2 between 12 $\%H_{2,vol}$ and UFL (kg). These are crucial parameters to compute the total combustion energy release, E. The solid lines represent the combination of vent pressure p and diameter d that results in a constant value of the metric of interest.

These maps provide an efficient way to visualize the results and can serve as a guide for vent design/consequence assessments where, given a set of constraints, one can provide the vent $p - d$ pair that would comply with this requirement. For example, the conditions that would limit the mass flow rate to be below 10 kg/s are vent diameters between 0.35 and 0.5 m, for decreasing vent source pressure of 2–1.3 bara.

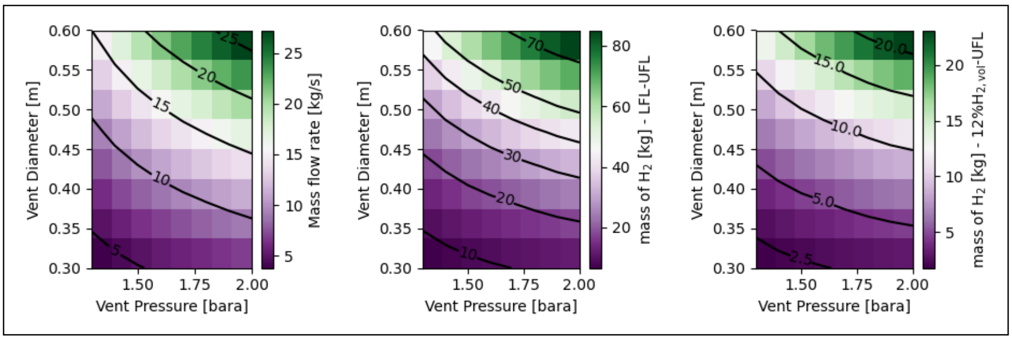

Figure 4 Dispersion results: heat maps showing relevant metrics that serve as inputs to the deflagration and detonation correlations.

3.3. OVERPRESSURE RESULTS

3.3.1. Unconfined uncongested deflagration

Quantities that can be computed based on the dispersion results such as the equivalent cloud radius, R_{cloud}, and the visible flame speed, V_f, that in turn enable to estimate the unconfined deflagration overpressure $P_2^* \ p_0$ using Equation 1 are shown in Figure 5. Clouds of ~ 8–18 m in radius are expected with associated values of V_f between 30 and 38 m/s. The overpressure is a decreasing function of distance; however, for ease of visualization and subsequent comparison with the detonation results, the latter is shown at a distance equal to the height of the vent (15 m) location that denotes the minimum distance to personnel or infrastructure in the process facility for which the venting scenarios are being investigated.

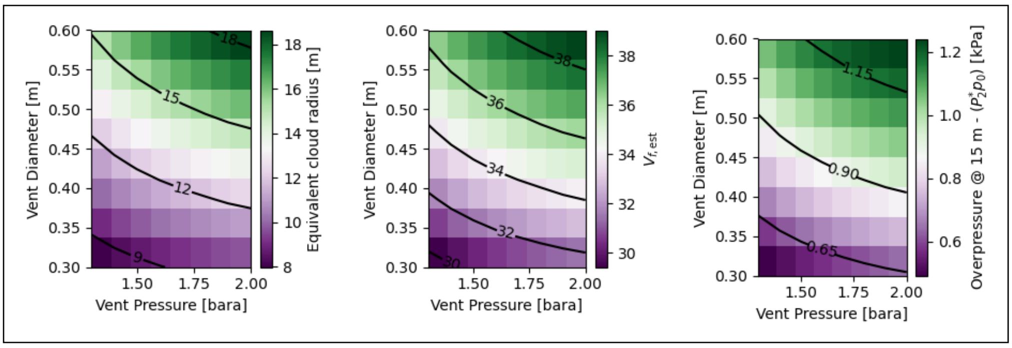

Figure 5 Heat maps of equivalent cloud radius, $R_{cloud} = (3V_{cloud}/2\pi)^{1/3}$ of a hemisphere containing the same volume as the entire release, estimated visible flame velocity, V_f, and estimated overpressure at 15 m computed using the unconfined uncongested deflagration correlation (Equation 1).

Higher overpressures are achieved for higher values of V_f since $P_2^* \propto (V_f/a_0)^2$; V_f is in turn proportional to $R^{1/3}$ which is satisfied for larger clouds as seen in Figure 5. The overpressures estimated for the conditions considered lie in the range of 0.49–1.24 kPa. Comparing these values against conditions for which experimental data exists—i.e., mostly horizontal releases at higher pressures, p = 24–400 bar, and smaller diameters, d = 6–52.5 mm (Daubech *et al.*, 2015, 2025; Groethe *et al.*, 2007; Takeno *et al.*, 2007; Blanchetière *et al.*, 2025)—suggests that the unconfined and uncongested deflagration correlation, as is, may be underestimating the overpressure values by at least an order of magnitude. Out of the 10 experimentally reported values, 5 lie below 10 kPa, and the remaining 5 data points are in the range of 20 and–57 kPa.

3.3.2. Unconfined uncongested detonation

Figure 6 shows the overpressure estimates for unconfined detonations at 15 m using Equation 3 for which the only input required from the dispersion calculations is the mass of H_2 between 12 $\%H_{2,vol}$ and UFL (or an alternative reasonable criterion to estimate the mass of

Hydrogen Safety
DOI: 10.58895/hysafe.51

H_2 that contributes to the blast loads). Again, the direct initiation of a detonation is unlikely in unconfined and uncongested nonuniform clouds; however, it is still useful to keep these estimates as an upper limit to the overpressure. The minimum and maximum values predicted for the range of conditions considered are 32.56 and 115 kPa, respectively.

Note the stark difference in overpressure estimates between the unconfined uncongested deflagrations and detonations correlations. There is clear room for improvement for the deflagration correlation to yield more realistic estimates, particularly given how sensitive the peak overpressure is to the visible flame velocity V_f, and the challenges in providing a sensible estimate for it from first principles in nonuniform, nonquiescent flammable clouds.

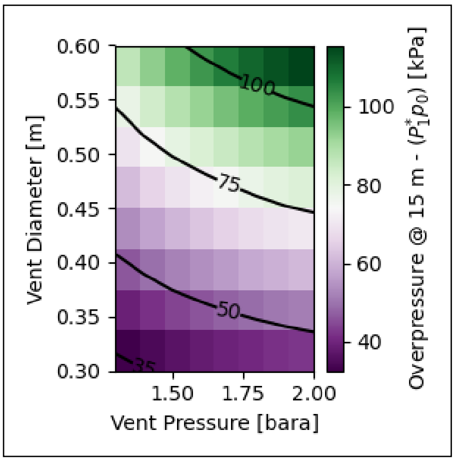

Figure 6 Heat map of estimated overpressure at 15 m computed using the unconfined uncongested detonation correlation (Equation 3).

3.4. DISCUSSION

While the conditions for which overpressure experimental data exists seem to lie mostly outside the parametric range considered herein, a way of verifying whether this is indeed the case is by computing the vent Reynolds number $Re = \rho U d/\mu$ where ρ and U are the gas density and velocity at the vent exit plane, respectively, and μ is the dynamic viscosity of the gas. The range of Re is $2.63 < Re \times 10^{-6} < 9.56$ as seen in the heat map in Figure 7. The Re computed from the vent source pressure and diameter reported in Groethe *et al*. (2007), Daubech *et al*. (2015, 2025), Takeno *et al*. (2007), and Blanchetière *et al*. (2025) are $Re \times 10^{-6}$ = 1.87, 2.06, 3.74, 7.93, 9.63, 20.6, and 24.2. The conditions in Daubech *et al*. (2015, 2025) (p = 40 bar; d = 12 mm) yield $Re \times 10^{-6} = 3.74$ with overpressures in the range of 6–20 kPa at 2 m. Groethe *et al*. (2007) (p = 24 bar; d = 42 mm) yield $Re \times 10^{-6} = 7.93$ with overpressures in the range of 4 kPa at 7 m. The differences in the reported values stem from the mass of H_2 released before the cloud was ignited.

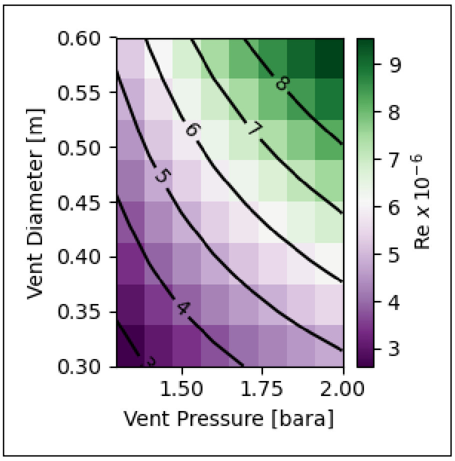

Figure 7 Reynolds number for the parametric space considered.

As mentioned above, one of the challenges in applying the methodology to realistic vent releases lies in the nonuniform, nonquiescent nature of the resulting flammable clouds. In the case of venting, the most plausible outcome upon delayed ignition of the release is for a flame to be initiated that subsequently accelerates consuming the cloud. The acceleration of the flame is responsible for the pressure buildup; hence, the visible flame velocity V_f is a crucial input to the deflagration correlation but difficult to estimate reliably. Note that Equation 2 is

Hydrogen Safety
DOI: 10.58895/hysafe.51

derived and validated for homogeneous quiescent clouds. V_f values are seldom reported in experimental campaigns; the work of Blanchetière *et al.* (2025), Daubech *et al.* (2015, 2025), Groethe *et al.* (2007), and Takeno *et al.* (2007) are exceptions to this rule.

Figure 8 (left) shows the V_f data plotted as a function of *Re*. A few extra points are added to the plot. Those reported by: (1) Pförtner and Schneider (1983) for quiescent hemispherical uniform clouds of size R = 10–14 m (stoichiometric H_2-air; Re = 0) to anchor V_f at no-flow to sensible values; (2) Miller, Eastwood, and Thomas (2015) for horizontal jets at p = 60 bar issuing from tubes of d = 20.9 and 52.5 mm. Overpressures were reported at two different locations per condition (with values ranging between 3.9 and 43 kPa) and sufficient information was provided to estimate the amount of H_2 released. The range of V_f that matched the experimentally reported values was iteratively computed using Equation 1. This allowed to increase the range of $V_f = f(Re)$ and observe whether a reasonable trend emerged in combination with the experimental data.

In Figure 8 (right), a curated dataset is shown. Three points were considered as outliers: (1) that of Takeno *et al.* (2007) (p = 400 bar; d = 10 mm) who report an unusually high V_f (978 m/s) that is more in line with the expected vent exit velocities for the given conditions (1098 m/s); (2) the reported maximum from Daubech *et al.* (2025) (510 m/s) since it differs from the maximum value reported by the same lead author in 2015 (280 m/s) for the same release conditions (p = 40 bar; d = 12 mm); (3) the reported maximum by Blanchetière *et al.* (2025). A least-squares regression line is fitted to the remaining data points given by $V_f = 6.0061Re + 110.0135$. With this, an improved V_f estimate for H_2 releases can be obtained.

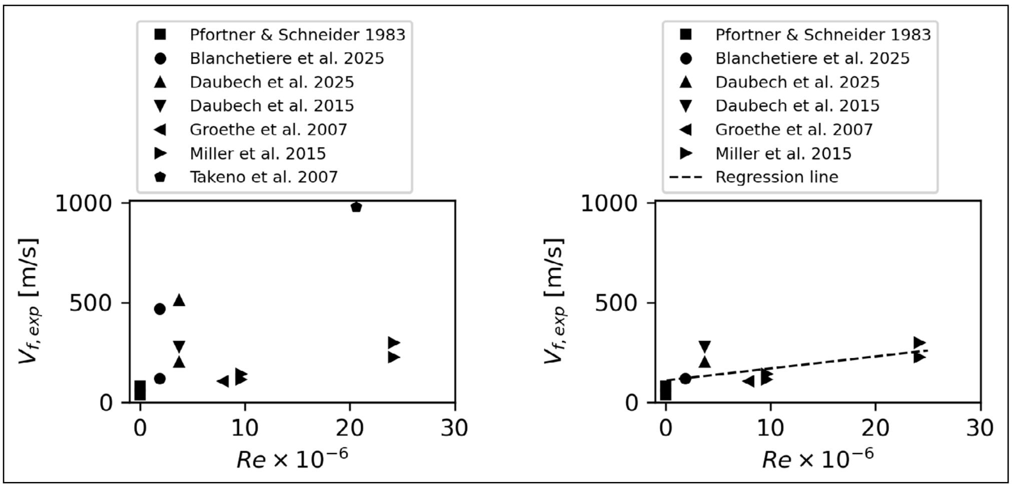

Figure 8 Measured visible flame velocity, V_f as a function of vent Reynolds number, *Re*. Left: complete dataset. Right: curated dataset. Dashed line is a least-squares regression line to the data points given by $V_f = 6.0061Re + 110.0135$.

Using the expression $V_f = f(Re)$, unconfined and uncongested deflagration overpressures are recomputed (see Figure 9). The overpressures at 15 m now range between 10 and 22 kPa for the parametric space considered. The values are significantly higher than the initial predictions shown in Figure 5 using Equation 2 to estimate V_f, but much lower than the unconfined uncongested detonation predictions, and more in line with the magnitudes of the experimental values reported in literature.

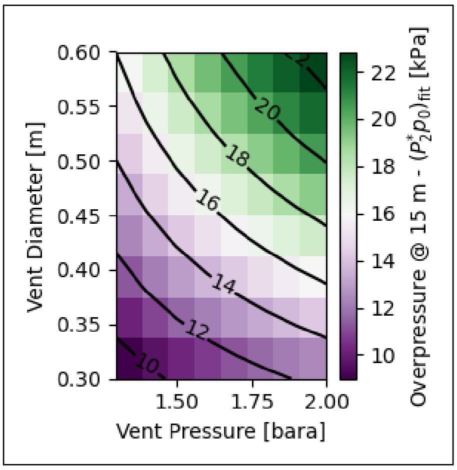

Figure 9 Unconfined uncongested deflagration results recomputed using the $V_f = f(Re)$ correlation derived from the experimental data.

4. CONCLUSION

A methodology for evaluating overpressures from unconfined and uncongested H_2 releases was developed, building on the approach introduced in Melguizo-Gavilanes, Pekalski, and Crerand (2024), and revisiting the work of Dorofeev (2007). The study proposed a straightforward method for estimating the amount of H_2 in flammable clouds that contributes to blast loads, using dispersion calculations performed with standard consequence modeling tools such as FRED and PHAST. A comparison of predicted overpressures with published experimental data revealed significant discrepancies: the unconfined and uncongested deflagration correlation tends to underpredict overpressures, whereas the detonation correlation overpredicts them. Since unconfined and uncongested, nonuniform, flammable clouds are unlikely to detonate directly, the focus was on refining the deflagration correlation to better align with experimental observations. The analysis highlighted that overpressure predictions were highly sensitive to the visible flame speed (V_f) used in the calculations—more so than to the mass of H_2 at a fixed V_f. However, estimating V_f from first principles is challenging due to the complex flow conditions typical of vent releases, such as nonuniform concentrations and background turbulence. A potential scaling relationship was identified in the data, showing that V_f could be expressed as a function of the vent Reynolds number ($V_f = f(Re)$). Incorporating this scaling into the deflagration correlation significantly improved the alignment of overpressure predictions with the values reported in the literature.

This work represents a step forward in developing a phenomenologically accurate and reliable correlation for vent overpressure predictions. However, several areas merit further exploration to advance and validate this research: (1) conducting additional large-scale experiments that incorporate vertical releases and account for actual or planned vent designs; (2) evaluating the updated methodology using data from the recent experimental campaigns conducted by Air Products in collaboration with BakerRisk, which focused on vertical releases (presented at GCPS by Shen *et al*. in April 2025); and (3) exploring the potential to unify low- and high-pressure release scenarios by analyzing overpressure data in vent Reynolds number and mass of H_2 space.

ACKNOWLEDGEMENTS

The authors would like to acknowledge the Erasmus HySET consortium (Project Reference: 101082651) for funding and support of the MSc project that is partially presented in this article.

COMPETING INTERESTS

The authors have no competing interests to declare.

AUTHOR AFFILIATIONS

Josue Melguizo-Gavilanes orcid.org/0000-0001-5174-6003
Shell Global Solutions B.V., Energy Transition Campus (ETCA), 1031 HW Amsterdam, The Netherlands

Adisa Jarubenjaluk
Shell Global Solutions B.V., Energy Transition Campus (ETCA), 1031 HW Amsterdam, The Netherlands

Andrzej Pekalski
Shell Research Limited UK, Shell Center, London SE1 7PB, United Kingdom

Andrew Crerand
Shell Research Limited UK, Shell Center, London SE1 7PB, United Kingdom

REFERENCES

Astbury, G. and **Hawksworth, S.J.** (2007) 'Spontaneous ignition of hydrogen leaks: a review of postulated mechanisms', *International Journal of Hydrogen Energy*, 32(13), pp. 2178–2185. Available at: https://doi.org/10.1016/j.ijhydene.2007.04.005

Bauwens, C.R.L. and **Dorofeev, S.B.** (2020) 'Modeling detonation limits for arbitrary non-uniform concentration distributions in fuel–air mixtures', *Combustion and Flame*, 221, pp. 338–345. Available at: https://doi.org/10.1016/j.combustflame.2020.08.003

Blanchetière, V., Armstrong, A., Wang, Y., Jambut, R., Wilkins, B. and **Salaün, N.** (2025) 'Delayed ignition of high-pressure hydrogen releases–experiments and engineering models', *Journal of Loss Prevention in the Process Industries*, 105589. Available at: https://doi.org/10.1016/j.jlp.2025.105589

Boivin, P., Le Boursicaud, M., Millán-Merino, A., Taileb, S., Melguizo-Gavilanes, J. and **Williams, F.** (2023) 'Hydrogen ignition and safety', In *Hydrogen for Future Thermal Engines*. Springer, pp. 161–236. Available at: https://doi.org/10.1007/978-3-031-28412-0_5

Brennan, S. and **Molkov, V.** (2013) 'Safety assessment of unignited hydrogen discharge from onboard storage in garages with low levels of natural ventilation', *International Journal of Hydrogen Energy*, 38(19), pp. 8159–8166. Available at: https://doi.org/10.1016/j.ijhydene.2012.08.036

Chamberlain, G., Oran, E. and **Pekalski, A.** (2019) 'Detonations in industrial vapour cloud explosions', *Journal of Loss Prevention in the Process Industries*, 62, p. 103918. Available at: https://doi.org/10.1016/j.jlp.2019.103918

Daubech, J., Hebrard, J., Jallais, S., Vyazmina, E., Jamois, D. and **Verbecke, F.** (2015) 'Un-ignited and ignited high pressure hydrogen releases: Concentration–turbulence mapping and overpressure effects', *Journal of Loss Prevention in the Process Industries*, 36, pp. 439–446. Available at: https://doi.org/10.1016/j.jlp.2015.05.013

Daubech, J., Hebrard, J. and **Leprette, E.** (2025) 'Influence of the flammable cloud geometry on the gas explosion effects', *Process Safety Progress*. Available at: https://doi.org/10.1002/prs.12674

Dorofeev, S. (1995) 'Blast effects of confined and unconfined explosions', *Proceedings of the 20th ISSW "Shock waves,"* pp. 77–86.

Dorofeev, S.B. (2007) 'Evaluation of safety distances related to unconfined hydrogen explosions', *International Journal of Hydrogen Energy*, 32(13), pp. 2118–2124. Available at: https://doi.org/10.1016/j.ijhydene.2007.04.003

Goodwin, G., Moffat, H., Schoegl, I., Speth, R. and **Weber, B.** (2023) *Cantera: An object-oriented software toolkit for chemical kinetics, thermodynamics, and transport processes*. Available at: https://www.cantera.org.

Groethe, M., Merilo, E., Colton, J., Chiba, S., Sato, Y. and **Iwabuchi, H.** (2007) 'Large-scale hydrogen deflagrations and detonations', *International Journal of Hydrogen Energy*, 32(13), pp. 2125–2133. Available at: https://doi.org/10.1016/j.ijhydene.2007.04.016

Kaneshige, M. and **Shepherd, J.E.** (1997) *Detonation database*.

Melguizo-Gavilanes, J., Pekalski, A. and **Cerand, A.** (2024) 'A methodology for hydrogen vents overpressure assessments', *Hazards 34 Process Safety Conference*, ICHEME, Manchester, UK.

Miller, D., Eastwood, C. and **Thomas, J.** (2015) 'Hydrogen jet vapor cloud explosion: test data and comparison with predictions', *Proceedings of the 11th Global Congress on Process Safety, AIChE Annual Meeting*, Austin, TX, pp. 26–30.

Oran, E.S., Chamberlain, G. and **Pekalski, A.** (2020) 'Mechanisms and occurrence of detonations in vapor cloud explosions', *Progress in Energy and Combustion Science*, 77, p. 100804. Available at: https://doi.org/10.1016/j.pecs.2019.100804

Pförtner, H. and **Schneider, H.** (1983) *Pnp-sichcrheitssofortprogramm, prozebgasfreisetzung-explosion in der gasfabrik und auswirkungen von druckwellen auf das containment*. Technical Report, Fraunhofer-ICT Internal Report.

Schefer, R., Houf, W., Williams, T., Bourne, B. and **Colton, J.** (2007) 'Characterization of high-pressure, underexpanded hydrogen-jet flames', *International Journal of Hydrogen Energy*, 32(12), pp. 2081–2093. Available at: https://doi.org/10.1016/j.ijhydene.2006.08.037

Shen, A., Miller, D., Lutostansky, E., Overa, S., Malik, D., Macon, K., Paschal, T. and **Thomas, J.** (2025) 'Hydrogen jet explosion: new tests, blast and fireball models', *Proceedings of the 21st Global Congress on Process Safety, Joint AIChE and CCPS Meeting*, Dallas, TX.

Smith, G.P., Golden, D.M., Frenklach, M., Moriarty, N.W., Eiteneer, B., Goldenberg, M., Bowman, C.T., Hanson, R.K., Song, S., Gardiner Jr, W.C. *et al.* (2021) *Gri-mech 3.0*. Available at: http://combustion.berkeley.edu/gri-mech/.

Stamps, D., Benedick, W.B. and **Tieszen, S.** (1991) *Hydrogen-air-diluent detonation study for nuclear reactor safety analyses*, Technical Report, Division of Systems, Nuclear Regulatory Commission, Washington, DC. Available at: https://doi.org/10.2172/6119703

Standard, A. (2020) *Pressure-relieving and depressuring systems*. American Petroleum Institute, p. 248.

Takeno, K., Okabayashi, K., Kouchi, A., Nonaka, T., Hashiguchi, K. and **Chitose, K.** (2007) 'Dispersion and explosion field tests for 40 MPa pressurized hydrogen', *International Journal of Hydrogen Energy*, 32(13), pp. 2144–2153. Available at: https://doi.org/10.1016/j.ijhydene.2007.04.018

Thomas, J.K., Eastwood, C. and **Goodrich, M.** (2015) 'Are unconfined hydrogen vapor cloud explosions credible?', *Process Safety Progress*, 34(1), pp. 36–43. Available at: https://doi.org/10.1002/prs.11685

Venetsanos, A., Papanikolaou, E. and **Bartzis, J.** (2010) 'The ADREA-HF CFD code for consequence assessment of hydrogen applications', *International Journal of Hydrogen Energy*, 35(8), pp. 3908–3918. Available at: https://doi.org/10.1016/j.ijhydene.2010.01.002

TO CITE THIS ARTICLE:
Melguizo-Gavilanes, J., Jarubenjaluk, A., Pekalski, A. and Crerand, A. (2026) 'Toward a Reliable Methodology for Assessing Overpressure in Hydrogen Vents', *Hydrogen Safety*, 3(1), pp. 63–72. Available at: https://doi.org/10.58895/hysafe.51

Submitted: 02 February 2026
Accepted: 04 February 2026
Published: 02 March 2026

KIT Scientific Publishing